Desalination and Water Treatment
www.deswater.com

doi: 10.5004/dwt.2019.23242

138 (2019) 99–112
January

Effect of depth of water on various efficiencies and productivity of *N* identical partially covered PVT collectors incorporated single slope solar distiller unit

Desh Bandhu Singh[a,*], Navneet Kumar[b], Harender[c], Satish Kumar[d], Sanjeev Kumar Sharma[e], Ashis Mallick[e]

[a]*Mechanical Engineering Department, Galgotias College of Engineering and Technology, Greater Noida, 201306, Uttar Pradesh, India, email: dbsiit76@gmail.com*

[b]*Mechanical Engineering Department, Galgotias College of Engineering and Technology, Greater Noida, UP, India*

[c]*Department of Mechanical Engineering, Shiv Nadar University, Greater Noida, UP, India*

[d]*Department of Civil Engineering, Indian Institute of Technology Delhi, HausKhas, New Delhi, 110016, India*

[e]*Department of Mechanical Engineering, Indian Institute of Technology (ISM), Dhanbad 826004 Jharkhand, India*

Received 26 December 2017; Accepted 2 October 2018

ABSTRACT

In the present investigation, various efficiencies and productivity of *N* identical partially covered PVT flat plate collectors integrated single slope solar distiller unit have been computed at different water depth under optimized condition to see the effect of variation of water depth on hourly and daily efficiencies and productivity. The meteorological data of 2 months: one belonging to winter season say January and the other belonging to summer season say June have been considered for New Delhi climatic condition. The hourly and daily thermal efficiencies, hourly and daily exergy efficiencies, hourly and daily electrical efficiencies, hourly and daily overall exergy efficiencies and hourly and daily productivities have been evaluated under optimized condition. It has been concluded that the increase in values of average daily efficiencies and productivity is significant till 1.4 m water depth.

Keywords: PVT; Active solar still; Efficiency; Productivity

1. Introduction

The proposed PVT collectors incorporated single slope solar distiller unit can be one of the best alternatives to palliate the present-day issue of shortage of clean water which is one of the basic requirements for the existence of life on the planet earth. This system is apposite for reducing water crisis problem in distant areas where solar radiation and contaminated water are present in plenty. The dynamic behavior of solar stills was first reported by Zaki et al. [1] under natural circulation mode whereas by forced circulation mode was first presented by Rai and Tiwari [2]. In forced mode operation, the rate of evaporation increases due to increase in heat transfer. Zaki et al. [2] stated that the active solar stills under forced mode operation on daily basis yield 24% higher with single collector when compared with conventional solar still. In active solar stills, a pump was deployed between the basin and the inlet of first collector with number of flat plate collectors (FPCs) connected in series.

Sathyamurthy et al. [3] have presented the detailed review of active solar distiller units till 2016. Tian et al. [4] have reviewed compound parabolic concentrator (CPC) for solar energy applications till 2017. Basin in active solar distillation system is provided with flat plate collector/ heat exchanger/evacuated tubular collector or concentrator collector. These devices are placed in basin to supply thermal energy with the help of external source. In heat exchanger generally water is used as fluid but sometimes based on the requirement other suitable liquid is used. Studies has also been made by integrating solar parabolic trough collector

* Corresponding author.

and a heat exchanger on solar still (SS) using single slope basin type [5]. The output efficiency of SS system was 18% more when it was compared with the conventional solar still. The enhancement in the SS system is due to rise in temperature of water in the basin which is done by imposing solar radiation and transferring heat from the exchanger installed in the basin. Circulation of fluid in the solar still to transfer heat to the bottom of solar still also helps in yield improvement significantly. Researchers suggested that there will be increase in potable water production by 9% if heat transfer rate is doubled [6]. There is a non-linear relationship between potable water production and heat transfer rate.

Badran et al. [7] introduced circulation operation by forced mode in double slope solar still basin type. From the above arrangement, they concluded that the potable water production is 52% higher than the one obtained from the conventional solar still. Taghvaei et al. [8] coupled FPC with SS for 10 d and evaluated for long-term execution. Further they suggested that depth of water should be higher because at higher depths, efficiencies of thermal and exergy is higher and also yield of potable water is higher due to the effect of heat storage. Calise et al. [9] developed an original tri-generation framework using PVT collectors for seawater desalination in European Mediterranean nations famous for plenty of renewable sources but needy in fossil fuels and water resources. Ibrahim et al. [10] modified the solar still by employed air cooled condenser externally and conveyed that the performance of modified solar still is increased in terms of potable water production (16.2%) and also in terms of thermal efficiency (29.7%) when compared with conventional solar still.

An experimental study of single slope solar still (SS) incorporated with two hybrid PVT collectors has been reported by Tiwari et al. [11] and Singh et al. [12] based on the work reported by Kumar and Tiwari [13]. Rufuss et al. [14] have performed techno-economic analysis using analytical hierarchy process and concluded that basin type solar still is one of the most efficient solar still. Rashidi et al. [15] have studied the performance of solar still by partitioning the basin and concluded that the yield of modified solar still was 8.16% higher than conventional solar still due to increased temperature difference between basin water and condensing cover. Malaeb et al. [16] investigated basin type solar still by inserting rotating drum in basin and concluded that the yield of modified solar still was higher than conventional solar still. Rabhi et al. [17] performed experiment on the single slope solar still which was modified by condenser and pin fins. From their study, it was found that the modified solar still yield was 41.98% higher than conventional solar still because temperature of water in the basin increases. The temperature of water increases because of absorber surface geometry. Sharshir et al. [18] developed hybrid solar still which incorporates humidification–dehumidification features in place of solar water heater and reported that hybrid solar distillation system yield was 200% more than a conventional solar still. The above results were achieved by reusing the water collected during humidification–dehumidification and feeding the water again back to solar still. Nguyen [19] studied the effect of various factors on the potable water yield of solar still and concluded that the potable water yield increase from 30% to 68% over the potable water yield of conventional solar desalination unit. Gnanaraj and Ramachandran [20] investigated SS incorporated with solar pond for optimization using Taguchi method and concluded that the optimum value of potable water yield could be obtained when the sodium chloride concentration level was 3.5 kg, the solar still was linked with lower converting zone of the pond, the reflecting angle at the bottom of the still was kept at 0° and the mirror at the pond at 135°. Yadav and Singh [21] investigated double exposure single basin solar still experimentally as well as theoretically and validated the theoretical values with experimental values. They reported values of correlation coefficient and root mean square deviation as 0.989 and 0.068, respectively.

Eltawil and Omara [22] investigated a single slope solar distiller unit which is integrated with collector, spraying unit and exterior condenser and reported that the developed solar still yield in the range from 51% to 148% making it superior to conventional solar still. Saeedi et al. [23] employed computational approach for PVT active solar still to find the optimal values as 7 and 0.044 kg/s for number of collectors and mass flow rate, respectively. Singh and Tiwari [24–27] did hypothetical research on climatic conditions of New Delhi using basin type solar stills which is incorporated with N identical PVT-CPC collectors. They reported that the double slope set up performed better than single slope set up of same configuration at 0.14 m under optimized condition due to higher energy, exergy and lower embodied energy for double slope set up. Further they suggested that when the depth of water in the basin was more than 0.31 m then the output for the single slope set up was superior to double slope PVT-CPC active solar still in terms of thermal efficiency, average daily productivity and overall thermal efficiency. An active solar distiller unit reported by Singh et al. [28] consists of the integration of evacuated tubes with the basin of SS worked in natural mode and they found that the exergy based efficiency was lying in the range of 0.15 to 8.25% at water depth of 0.03 m during an archetypal day of summer meteorological situation. Further, Kumar et al. [29] reported the similar set up in forced mode and they found that the daily yield of potable water was 3.47 kg at 0.01 m water depth for meteorological situation of New Delhi. A similar attempt was reported by Singh and Tiwari [30] in which N number of identical evacuated tubular collectors was added to the basin of SS. They developed characteristic equations for the system. Singh and Tiwari [31] have studied energy, exergy and cost analyses of basin type solar still coupled with ETCs and concluded that the production cost of potable water is lower for double slope active solar still due to higher yield at 0.14 m water depth. In this work, exergo-economic and enviro-economic analyses of SS integrated with N identical ETCs have been carried out. Arunkumar et al. [32] have studied compound parabolic concentrator tubular solar distiller units experimentally and they have reported a daily yield of 2.9 L/m^2.

The extant research represents that the effect of water depth on the performance of single slope solar distiller unit incorporated with N identical flat plate collectors has not been reported by any researchers. In this work, N identical partially covered PVT collectors integrated single slope solar distiller unit has been analyzed to know the effect of the variation of water depth on the performance of proposed active solar still. The objective of the proposed investigation can be stated as follows:

- To compute various hourly efficiencies and hourly productivity at different water depths to see the effect of variation of depth of water on hourly efficiencies and hourly productivity under optimized condition.
- To compute various daily efficiencies and daily productivity at different water depths to see the effect of variation of depth of water on daily efficiencies and daily productivity under optimized condition.

2. System description

Figs. 1(a)–(c) represent schematic diagram of the proposed N-PVT-FPC-SS, cross sectional side view of the first partially covered PVT-FPC and cut section XX′ front view of the first partially covered PVT-FPC. Table 1 shows the specifications of N-PVT-FPC-SS. At low temperatures, discharge is higher when collectors arranged in parallel whereas at high temperatures, discharge is low when collectors arranged in series. In the present study, collectors arranged in series are considered in order to get water temperature higher in the basin.

When connection is in series, outlet of each partially covered PVT-FPC is connected to the inlet of its successive partially covered PVT-FPC. A closed loop concept has been used in the present study in which the pump pumps the water from the basin into the inlet of first PVT-FPC and discharges the hot water into the basin available at the outlet of *N*th PVT-FPC. All the collectors are arranged in series and provided with a 30° inclination angle so that the set up can capture maximum solar radiation in a year. PVT provides the power source for DC motor pump. The pump has been provided to overcome the pressure drop to confirm smooth circulation of water throughout the system.

The single slope active solar distiller unit in this study is finished with glass reinforced plastic with 2 m^2 effective area of basin. To get maximum annual solar intensity, the active solar still is installed facing south direction. A transparent glass having inclination of 15° with the horizontal surface has been used as condensing cover. In order to absorb maximum share of solar flux, black paint has been applied on the inner surfaces of bottom and side walls of solar still. Window-putty is used to seal the joint of glass with the basin. In the

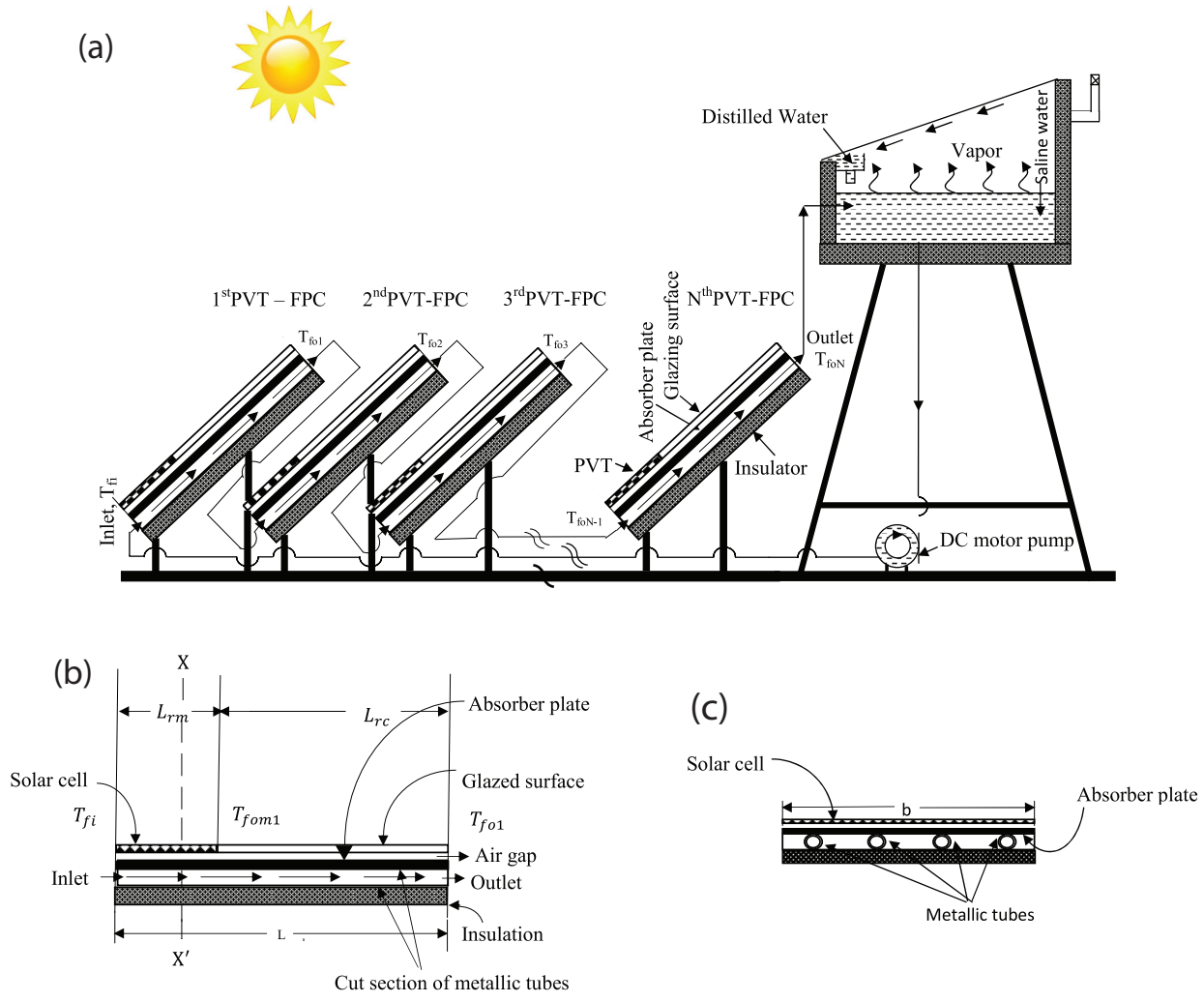

Fig. 1. (a) Single slope solar still incorporated with N identical partially covered PVT-FPC. (b) Cross section side view of the first partially covered PVT-FPC. (c) Cut section XX′ front view of the first partially covered PVT-FPC.

Table 1
Specifications of single slope solar still incorporated with *N* identical partially covered PVT flat plate collectors

Component	Specification	Component	Specification
Single slope active solar still			
Length	2 m	Orientation	South
Width	1 m	Thickness of glass cover	0.004 m
Inclination of glass cover	15°	K_g	0.816 W/m K
Height of smaller side	0.2 m	Thickness of insulation	0.1m
Material of body	GRP	Thermal conductivity of insulation	0.166 W/m K
Material of stand	GI	ε_w	0.82
Cover material	Glass	ε_g	0.92
PVT-FPC collector			
Type and no. of collectors	Tube in plate type, N	Area of module	0.25 m × 1.0 m
Area of solar collector	1.0 m × 1.0 m	F'	0.968
Collector plate thickness	0.002	τ_g	0.95
Thickness of copper tubes	0.00056 m	α_c	0.9
Length of each copper tubes	1.0 m	β_c	0.89
Thickness of insulation	0.1 m	α_P	0.8
Angle of FPC with horizontal	30°	K_i (W m^{-1} K^{-1})	0.166
Thickness of toughen glass on FPC	0.004 m	FF	0.8
Effective area of collector under glass	0.75 m^2	Pipe diameter	0.0125 m
DC motor rating	12 V, 24 W		

rear wall of the solar still, an opening is provided through which saline/brackish water is fed into the basin. For the maintenance of the set-up, another opening is provided at the bottom of the basin through which cleaning can be done whenever required. The complete set up is fixed on an iron stand.

The transparent glass reflects from the outer surface and partially absorbs the solar flux impinging on it and transmits the rest of the solar flux to the water in the basin. After that, the water mass too reflects and absorbs some portion of the received solar flux and transmits the rest to the basin liner. The radiation of solar falling on the surface of basin liner will be on its surface and heat will be transferred to the basin causing the water temperature to increase further. In the basin, water evaporation takes place due to the temperature differences between the basin water and inner surface of condensing cover. The water which gets evaporated undergoes film-type condensation and this condensed water drops down and collected through the channel and is tapped off to an external container.

3. Mathematical formulation

The useful heat gain from N-PVT-FPCs and temperature at the outlet of the last collector (*N*th collector) can be written as follows [33,34]:

$$\dot{Q}_{u,N} = N\left(A_m + A_c\right)\left[\left(\alpha\tau\right)_{\text{eff},N} I\left(t\right) - U_{L,N}\left(T_{\text{fi}} - T_a\right)\right] \tag{1}$$

$$T_{\text{foN}} = \frac{\left(AF_R\left(\alpha\tau\right)\right)_1}{\dot{m}_f C_f}\frac{\left(1-K_k^{\,N}\right)}{\left(1-K_k\right)} I\left(t\right) + \frac{\left(AF_R U_L\right)_1}{\dot{m}_f C_f}\frac{\left(1-K_k^{\,N}\right)}{\left(1-K_k\right)} T_a + K_k^N T_{\text{fi}} \tag{2}$$

where T_{foN} stands for temperature at the outlet of last collector (*N*th collector) and T_{fi} stands for temperature at the inlet of first collector. The variable T_{fi} can be taken as identical to T_w because water from the basin is compelled to go into the inlet of the first collector with the help of pump due to the formation of closed loop with basin. Also, heated water available at the outlet of last collector (*N*th collector) is made to flow to the basin of solar still. Hence, the variable T_{wo} can be taken identical to T_{foN}. Various unknown terms in Eqs. (1) and (2) have been presented in Appendix A.

The analytical expression for electrical efficiency [35,36] of solar cells (η_{cN}) of *N* identical PVT-FPC can be computed as:

$$\eta_{\text{cN}} = \eta_o\left[1 - \beta_o\left(\bar{T}_{\text{cN}} - T_o\right)\right] \tag{3}$$

where η_o stands for the efficiency at standard test condition. The emblem $\bar{T}_{cN}$ stands for the mean value of solar cell temperature of *N*th collector and its value can be calculated using the relation reported by Shyam et al. [34] in which T_{fi} is identical to T_w as series connected collectors have been put to form a closed loop with basin.

Ensuing Singh et al. [12], one can write energy balance equations for all elements of the proposed system and these equations in combination with Eq. (1) can be rearranged and

consequently solved using boundary condition to obtain expressions for water temperature (T_w), glass cover temperature (T_{gi} and T_{go}) and hourly production of potable water as follows:

$$T_w = \frac{\bar{f}(t)}{a}\left(1-e^{-at}\right)+T_{w0}e^{-at} \tag{4}$$

$$T_{gi} = \frac{\alpha_g' I_s(t) A_g + h_{1w} T_w A_b + U_{c,ga} T_a A_g}{U_{c,ga} A_g + h_{1w} A_b} \tag{5}$$

$$T_{go} = \frac{\frac{K_g}{L_g} T_{gi} + h_{1g} T_a}{\frac{K_g}{L_g} + h_{1g}} \tag{6}$$

The hourly distillate output ($\dot{m}_{ew}$) from solar still can be computed as:

$$\dot{m}_{ew} = \frac{h_{e,wg} A_b \left(T_w - T_{gi}\right)}{L} \times 3600 \tag{7}$$

where L stands for the latent heat of evaporation. It can be evaluated by following the relations reported by Fernandez and Chargoy [37] and Toyama and Kagakuv [38].

The different terms used in Eqs. (4) to (6) have been presented in Appendix A.

4. Analysis

The following performance parameters for N-PVT-FPC-SS systems have been computed.

4.1. Thermal efficiency

First law of thermodynamics has been used to compute thermal efficiency. Following Tiwari [39], the hourly thermal efficiency for single and double slope PVT-FPC active solar distillation system can be written as follows:

$$\eta_{hourly,thermal} = \frac{\dot{m}_{ew} \times L}{\left[\dot{Q}_{uN}(t) + A_b \times I_s(t)\right] \times 3600} \times 100 \tag{8}$$

Following Eq. (8), daily thermal efficiency for N-PVT-FPC-SS can be written as follows:

$$\eta_{daily,thermal} = \frac{\sum_{t=1}^{24} \dot{m}_{ew} \times L}{\sum_{t=1}^{24}\left[\dot{Q}_{uN}(t) + A_b \times I_s(t)\right] \times 3600} \times 100 \tag{9}$$

The value of solar intensity used in Eq. (9) is zero during off sunshine periods. But, the potable water yield will be there during off sunshine periods also because of the heat content stored in water mass during sunshine periods.

4.2. Thermal exergy efficiency

Following Nag [40], the hourly thermal exergy output ($\dot{E}x_c(t)$) from N identical PVT-FPC can be expressed as follows:

$$\dot{E}x_c(t) = \left(\dot{m}_f \times C_f\right)\left[\left(T_{foN} - T_{fi}\right) - (T_a + 273) \times \ln\frac{(T_{foN} + 273)}{(T_{fi} + 273)}\right] \tag{10}$$

Here, $\dot{m}_f$, C_f, T_{foN}, T_{fi} and T_a stands for the flow of fluid mass per unit time through PVT-FPC, heat capacity for unit mass of fluid flowing through collector, temperature at the exit of Nth PVT-FPC, temperature at the inlet of 1st PVT-FPC and ambient temperature respectively.

Following Eq. (10), the hourly output thermal exergy $\dot{E}x_{out,SS}(W)$ for single slope PVT-FPC active solar distillation system can be expressed as follows (Cooper [41]; Dunkle [42]):

$$\dot{E}x_{out} = A_b h_{ewg}\left[\left(T_w - T_{gi}\right) - (T_a + 273) \times \ln\left\{\frac{(T_w + 273)}{(T_{gi} + 273)}\right\}\right] \tag{11}$$

$$\text{where } h_{ewg} = 16.273 \times 10^{-3} h_{cwg}\left[\frac{P_w - P_{gi}}{T_w - T_{gi}}\right] \text{ (Cooper, 1973)} \tag{12}$$

$$\text{where } h_{cwg} = 0.884\left[\left(T_w - T_{gi}\right) + \frac{\left(P_w - P_{gi}\right)T_w}{268.9 \times 10^3 - P_w}\right]^{\left(\frac{1}{3}\right)} \text{ (Dunkle, 1961)}$$

$$P_w = \exp\left[25.317 - \frac{5144}{(T_w + 273)}\right] \text{ and}$$

$$P_{gi} = \exp\left[25.317 - \frac{5144}{(T_{gi} + 273)}\right]$$

Hence, hourly thermal exergy efficiency of single and double slope PVT-FPC active solar distillation system can be expressed as follows:

$$\eta_{hourly,exergy} = \frac{\dot{E}x_{out,s}(t)}{\dot{E}x_c(t) + 0.933 \times \left(A_b \times I_s(t)\right)} \times 100 \tag{13}$$

Here, the factor 0.933 has been obtained using the expression given by Petela [43]. It has been used to convert radiation to exergy.

Following Eq. (13), the daily thermal exergy efficiency of N-PVT-FPC-SS can be written as follows:

$$\eta_{daily,exergy} = \frac{\sum_{t=1}^{24}\left[\dot{E}x_{out,s}(t)\right]}{\sum_{t=1}^{24}\left[\dot{E}x_c(t) + 0.933 \times \left(A_b \times I_s(t)\right)\right]} \times 100 \tag{14}$$

4.3. Electrical exergy efficiency

The hourly electrical energy/electrical exergy ($\dot{E}x_e$) for the system can be written as follows:

$$\dot{E}x_e = A_m I(t)\sum_{1}^{N}(\beta_c \tau_g \eta_{cN}) \tag{15}$$

Following Tiwari et al. [11], the electrical exergy efficiency of N-PVT-FPC-SS can be expressed as follows:

$$\eta_{\text{hourly,electrical exergy}} = \frac{\dot{E}x_e(t) - \dot{P}_u(t)}{0.933 \times A_m \times N \times I(t)} \times 100 \tag{16}$$

$$\eta_{\text{daily,electrical exergy}} = \frac{\sum_{t=1}^{24}\left(\dot{E}x_e - \dot{P}_u\right)}{0.933 \times \sum_{t=1}^{t=24}\left[A_m \times N \times I(t)\right]} \times 100 \tag{17}$$

Here $\dot{P}_u(t)$, N, $I(t)$ and A_m are hourly consumption of pump, number of collectors, radiation falling on collector and area of module respectively. Hourly electrical exergy ($\dot{E}x_e(t)$) can be computed using Eq. (15). The value of radiation falling on collector and electrical energy/exergy are zero during off sunshine hours.

4.4. Overall exergy efficiency

Overall exergy represents the summation of thermal exergy and electrical exergy. Following Huang et al. [44], the hourly overall exergy efficiency of N-PVT-FPC-SS can be written as follows:

$$\eta_{\text{hourly,overall exergy}} = \frac{\dot{E}x_{\text{out},s}(t) + \left(\dot{E}x_e(t) - \dot{P}_u(t)\right)}{0.933 \times \left[\left(A_b \times I_s(t)\right) + (A_m + A_c) \times N \times I(t)\right]} \times 100 \tag{18}$$

Following Eq. (18), the daily overall exergy efficiency of N-PVT-FPC-SS can be written as follows:

$$\eta_{\text{daily,overall exergy}} = \frac{\sum_{t=1}^{24}\left[\dot{E}x_{\text{out},s}(t) + \left(\dot{E}x_e(t) - \dot{P}_u(t)\right)\right]}{0.933 \times \sum_{t=1}^{24}\left[\left(A_b \times I_s(t)\right) + \left(A_m + A_c\right) \times N \times I(t)\right]} \times 100 \tag{19}$$

where the values of electrical exergy and solar flux used in Eqs. (16)–(19) are zero during off sunshine hours.

4.5. Hourly and daily productivity

Following ILO [45], the hourly productivity for N-PVT-FPC-SS can be written as follows:

$$\text{Hourly productivity} = \frac{\left(\text{Hourly yield} \times (\text{SP})_w\right) + \left(\text{Hourly electricity gain} \times (\text{SP})_e\right)}{\text{Hourly cost}} \times 100 \tag{20}$$

The hourly yield used in Eq. (20) can be computed using Eq. (7). The daily yield can be obtained by adding hourly yield for 24 h and daily electricity gain can be obtained by adding hourly electricity gain for 10 h as electricity is generated during sunshine hours only. Hence, daily productivity for N-PVT-FPC-SS can be expressed as follows:

$$\text{Daily productivity} = \frac{\left(\text{Daily yield} \times (\text{SP})_w\right) + \left(\text{Daily electricity gain} \times (\text{SP})_e\right)}{\text{Daily cost}} \times 100 \tag{21}$$

The daily cost can be calculated by dividing uniform end-of-year annual cost (UAC) with 365 d and the hourly cost can be calculated by dividing daily cost with 24 h. UAC is based on present value method and it can be written as follows:

$$\text{UAC} = P_s \times F_{\text{CR},i,n} + \text{M} \times F_{\text{CR},i,n} - S_s \times F_{\text{SR},i,n} \tag{22}$$

The maintenance cost (M) is expressed as the multiplication of the net present cost (P_s) and maintenance cost factor which is generally taken as 0.1. The expression for various terms used in Eq. (20) is given in Singh and Tiwari [31].

5. Methodology

The following methodology has been implemented for the computation of various performance parameters N-PVT-FPC-SS.

5.1. Step I

The meteorological data for 2 months: one belonging to summer season say June and the other belonging to winter season say January has been deliberated for the calculation of parameters namely efficiency and productivity of N-PVT-FPC-SS. Solar intensity on the horizontal surface and atmospheric temperature have been taken from Indian Meteorological Department, Pune, India. The values of solar intensity on the surface having inclination of certain angle with the horizontal at 30° north latitude have been computed using computational program written in MATLAB.

5.2. Step II

The variables $\dot{Q}_{uN}(t)$ and T_{foN} have been computed with the help of Eqs. (1) and (2), respectively. Then, variables η_{cN} and $\bar{T}_{cN}$ have been evaluated using the relation reported by Singh and Tiwari [24] in which T_{fi} is identical to T_w because series connected collectors are in closed loop with the basin of solar still in the system under consideration.

5.3. Step III

Water temperature, glass temperature and hourly yield for N-PVT-FPC-SS have been evaluated using Eqs. (4)–(7).

5.4. Step IV

The hourly thermal, daily thermal, hourly exergy, daily exergy, hourly electrical exergy, daily electrical exergy, hourly overall exergy, daily overall exergy and hourly overall efficiencies for N-PVT-FPC-SS have been evaluated using Eqs. (8), (9), (13), (14), (16), (17)–(19), respectively. The hourly and daily productivities have been computed using Eqs. (20) and (21), respectively. Further, the average daily efficiencies and average daily productivity have been computed considering 2 months namely June (summer) and January (winter) at different water depths to assess the effect of water depth on the performance of N-PVT-FPC-SS.

6. Results and discussion

All pertinent equations and data for solar radiation, ambient temperature and average velocity have been fed to MATLAB. Total radiation on horizontal surface and ambient temperature are represented by Fig. 2. The values of average velocity have taken as 2.77 and 4.11 m/s for January and June, respectively. The output obtained is shown in Figs. 3–18.

The variable $T_{foN,max}$ has been plotted against N at given mass flow rate ($\dot{m}_f$) for N-PVT-FPC-SS for an archetypal day of June month. The supply of heat per unit time ($\dot{Q}$) by a number of series connected FPCs to the basin of N-PVT-FPC-SS can be expressed as $\dot{Q} = \dot{m}_f C_f (\Delta T_f)$; where $\Delta T_f = T_{foN} - T_{fi}$. From this relation, one can conclude that the amount of heat supplied to the basin is directly proportional to $\dot{m}_f$, that is, higher the value of $\dot{m}_f$, higher will be the value of rate of heat supplied to the basin. However, the value of T_{foN} has been found to decrease with rise in the value of $\dot{m}_f$ because less time is accessible to liquid in the collector to engross heat. The amount of heat loss from absorber increases with the increase in the value of $\dot{m}_f$. Hence, there is a need to compromise between the value of $\dot{m}_f$ and T_{foN}.

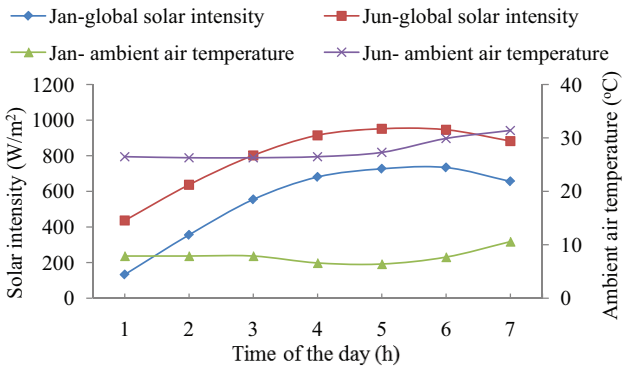

Fig. 2. Hourly variation of radiation on horizontal surface and ambient air temperature for January and June.

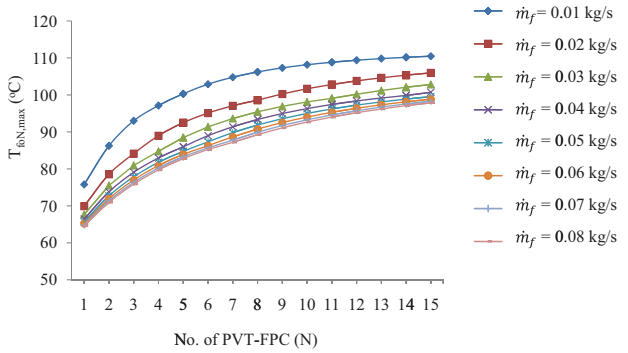

Fig. 3. Variation of maximum temperature of water in the collector ($T_{foN,max}$) for N-PVT-FPC-SS for a typical day in the month of June.

Fig. 3 represents that the distance between curves decreases with the increase in the value of $\dot{m}_f$ and the distance between curves becomes insignificant beyond $\dot{m}_f$ = 0.016 kg/s. Also, slope of curves is found to decrease with the increase in value of $\dot{m}_f$ and it becomes insignificant beyond $\dot{m}_f$ = 0.016 kg/s. It means that the change in value of T_{foN} for a given mass flow rate becomes insignificant if N is increased for $\dot{m}_f \geq 0.016$ kg/s. Hence, optimum value of $\dot{m}_f$ is 0.016 kg/s. Further, daily yield of potable water increases as the value of N is increased at $\dot{m}_f$ = 0.016 kg/s as can be observed from Fig. 8. One can, however, not go beyond N = 12 as the value of T_{foN} becomes more than the boiling point of water, that is, 100°C for $N > 12$ at $\dot{m}_f$ = 0.016 kg/s as evident from Fig. 3. So, the optimum value of N for N-PVT-FPC-SS is 12.

Fig. 4 represents the plot of hourly thermal efficiency for N-PVT-FPC-SS against time at optimum values of N and $\dot{m}_f$ for an archetypal day in June month. Fig. 5 represents the similar plot for January month. Values of hourly thermal efficiency for N-PVT-FPC-SS have been found to decrease as the value of water depth is increased which resembles the

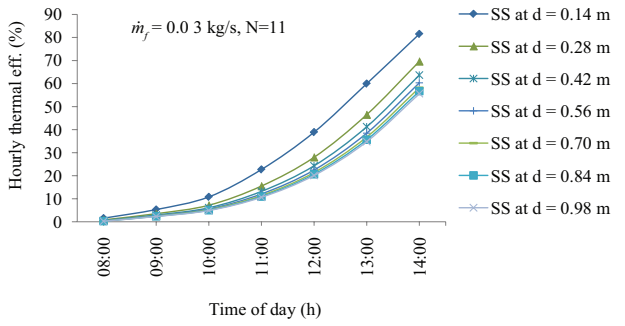

Fig. 4. Variation of hourly thermal efficiency of N-PVT-FPC-SS for a typical day in the month of June.

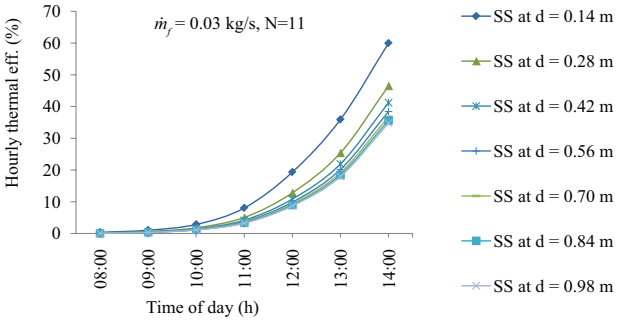

Fig. 5. Variation of hourly thermal efficiency of N-PVT-FPC-SS for a typical day in the month of January.

expectation. It has been found to occur because of the fact that the value of T_w decreases as the value of water depth is increased and hence, lower temperature difference between water and glass cover is obtained at higher depth of water resulting in lower yield during sunshine hours (day time). Fig. 6 shows the variation of average (January and June) daily thermal efficiency with depth of water for N-PVT-FPC-SS. It is observed that the curve becomes approximately horizontal after 1.40 m water depth. It means the optimum value of water depth is 1.40 m on the basis of average daily thermal efficiency. However, the system becomes too bulky at this water depth and further study is required to operate at this depth.

The variation of hourly exergy efficiency for N-PVT-FPC-SS at optimum values of N and $\dot{m}_f$ for an archetypal day in June month has been presented in Fig. 7. Fig. 8 presents the similar plot of January month. The hourly exergy efficiency has been found to decrease as the water depth increases during sunshine hours as expected. The reason being that temperature of water mass decreases with the increase in depth and lower temperature difference between water and glass cover is obtained at higher depth of water resulting in lower exergy gain at increased water depth during sunshine hours (day time). Also, exergy represents the quality of energy and lower exergy is gained at lower temperature because of higher loss. The plot of average daily exergy efficiency of N-PVT-FPC-SS with depth of water has been presented in Fig. 9. The value of average daily exergy efficiency has been found to increase with the increase in water depth till 1.40 m and then the value of average daily exergy efficiency becomes almost constant. It suggests that 1.40 m water depth can be taken as the optimum water depth on the basis of average exergy efficiency. But, the solar distiller unit turns out to be bulky at such a high value of water depth. Hence, further study is required to operate at this water depth.

The plot of hourly electrical exergy efficiency of the proposed solar distiller unit for an archetypal day in June month has been shown in Fig. 10. Fig. 11 shows the similar plot for January month. The value of hourly exergy efficiency has been found to increase first and then to decrease. The value of hourly electrical exergy efficiency has been found to increase due to increase in the value of solar intensity. But, the value of hourly electrical exergy efficiency again decreases due to increased temperature at higher values of solar intensity as the number of collisions increases at higher temperatures.

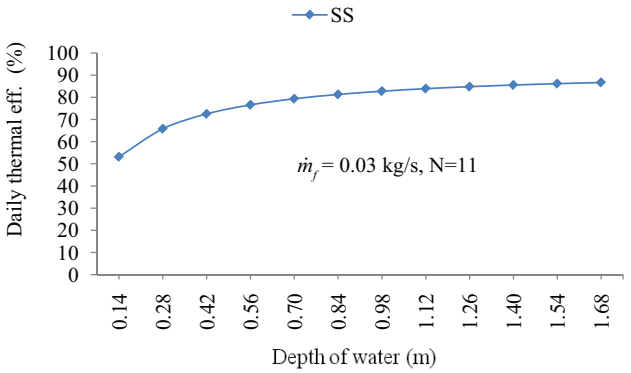

Fig. 6. Variation of average daily thermal efficiency with depth of water of N-PVT-FPC-SS.

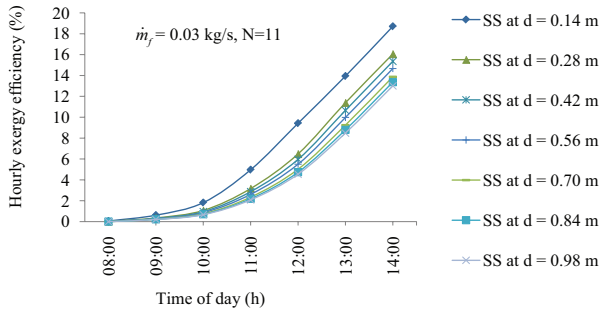

Fig. 7. Variation of hourly exergy efficiency of N-PVT-FPC-SS for a typical day in the month of June.

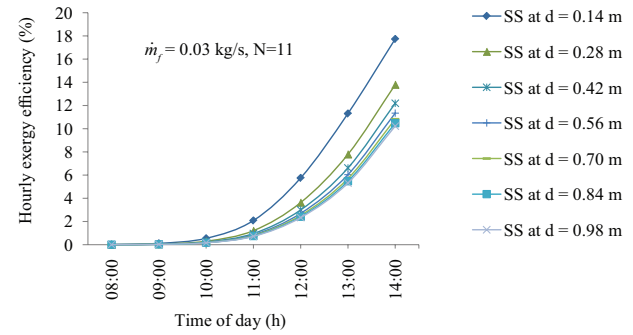

Fig. 8. Variation of hourly exergy efficiency of N-PVT-FPC-SS for a typical day in the month of January.

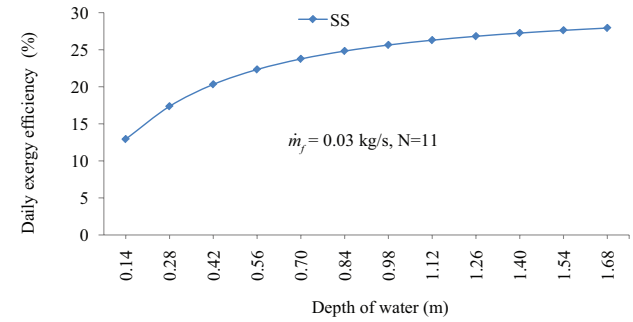

Fig. 9. Variation of average daily exergy efficiency with depth of water of N-PVT-FPC-SS.

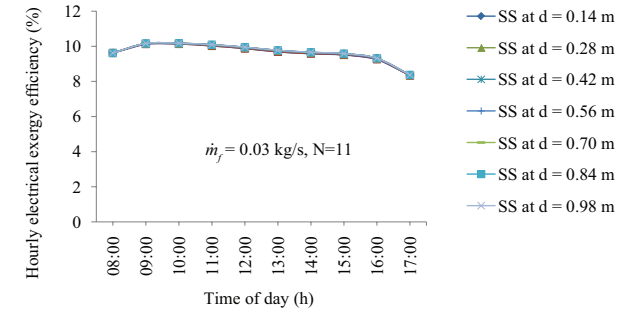

Fig. 10. Variation of hourly electrical efficiency of N-PVT-FPC-SS for a typical day in the month of June.

The increased number of collisions increases the resistance and hence lower exergy efficiency. The plot of average daily exergy efficiency for N-PVT-FPC-SS has been shown in Fig. 12. The value of average daily exergy efficiency has been found to be almost same at all water depth as expected because temperature of photovoltaic module remains almost constant.

The plot of hourly overall exergy efficiency for N-PVT-FPC-SS at optimum values of N and $\dot{m}_f$ for an archetypal day in June month is shown in Fig. 13. The similar plot is shown in Fig. 14 for January month. The value of hourly overall exergy efficiency for N-PVT-FPC-SS has been found to decrease as the value of water depth increases during sunshine hours

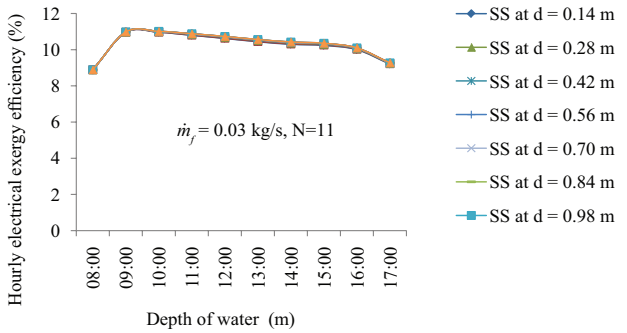

Fig. 11. Variation of hourly electrical efficiency of N-PVT-FPC-SS for a typical day in the month of January.

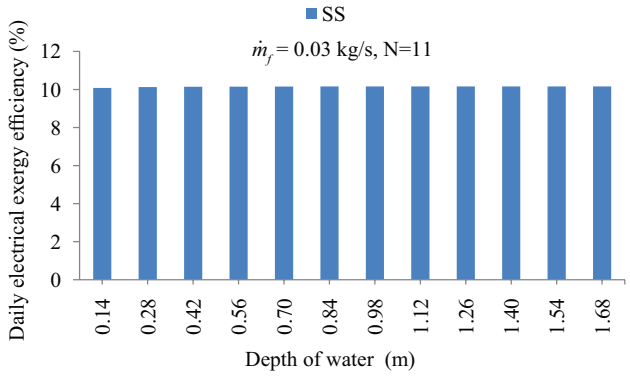

Fig. 12. Variation of average daily electrical exergy efficiency with depth of water for N-PVT-FPC-SS.

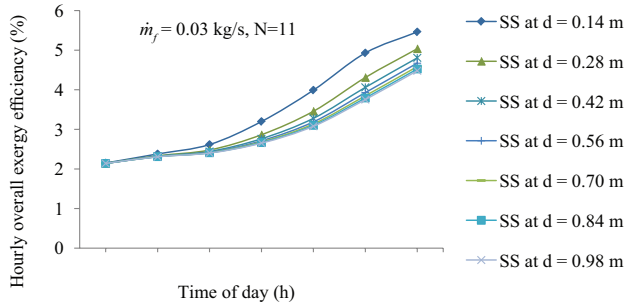

Fig. 13. Variation of hourly overall exergy efficiency of N-PVT-FPC-SS for a typical day in the month of June.

as increase in temperature of water is less at higher water depth. Fig. 15 shows the plot of average overall daily exergy efficiency with water depth for N-PVT-FPC-SS under optimized condition. The value of average overall daily exergy efficiency has been found to increases till 1.40 m water depth and then it becomes almost constant. It suggests that the optimal water depth for N-PVT-FPC-SS is 1.4 m on the basis of overall daily exergy efficiency. But, the proposed solar distiller unit at such a high value of water depth turns out to be bulky as mentioned earlier. Hence, further study is required to operate at such high value of water depth. The value of average daily overall exergy efficiency has been found to be almost constant after 1.40 m water depth due to the fact that the temperature of water does not rise much beyond 1.40 m water depth due to increased water mass in the basin at higher water depth.

The plot of hourly productivity with the variation in water depth of N-PVT-FPC-SS for a typical day in June month has been shown in Fig. 16. The similar plot has been shown in Fig. 17 for January month. The rate of interest and life of system have been taken as 5% and 50 years, respectively, for the computation of uniform end-of-year annual cost. Selling price of water per kg and selling price of electricity per kWh have been taken as X 5 and ₹ 4, respectively. Table 2 represents the capital investment for N-PVT-FPC-SS. Eq. (24) has been used to compute UAC. The values of UAC have been presented in Table 3. The value of hourly productivity for N-PVT-FPC-SS has been found to decrease with the

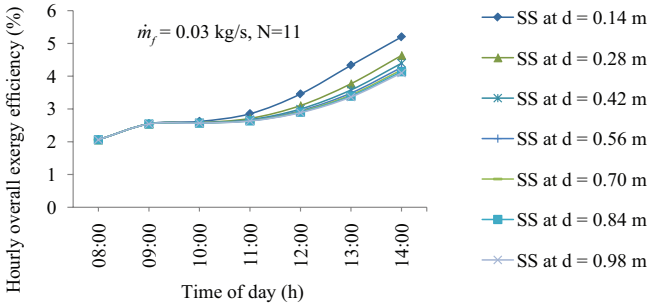

Fig. 14. Variation of hourly overall exergy efficiency of N-PVT-FPC-SS for a typical day in the month of January.

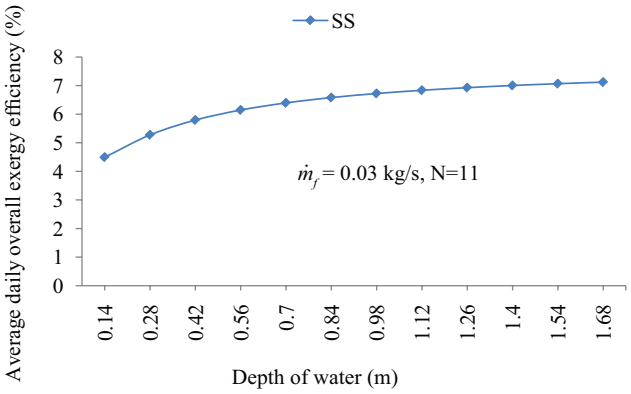

Fig. 15. Variation of average overall daily exergy efficiency of N-PVT-FPC-SS.

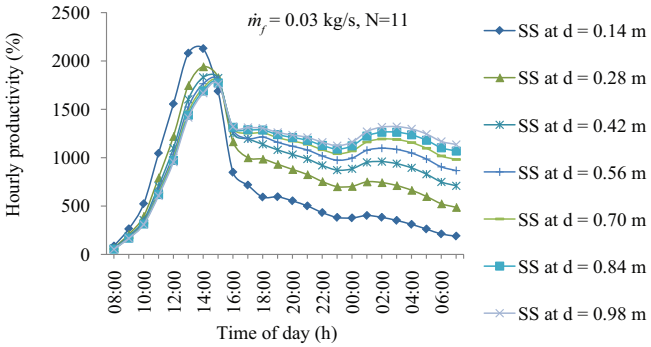

Fig. 16. Variation of hourly productivity with depth of water for N-PVT-FPC-SS for a typical day in the month of June.

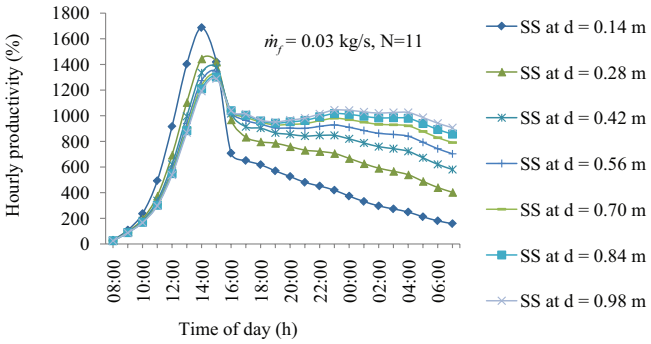

Fig. 17. Variation of hourly productivity with depth of water of N-PVT-FPC-SS for a typical day in the month of January.

Table 2
Capital investment for N-PVT-FPC-SS

S. No.	Parameter	Cost (₹)
1	Solar still	23,143
2	*N* identical PVT collectors (*N* = 11)	93,500
3	Motor and pump	1,000
4	Fabrication cost	6,000
5	Salvage value of the system after 50 years, if inflation remains at 4% in India (using present value of scrap material sold in Indian market)	82,895

increase in the value of water depth during sunshine hours (day) and the value of the hourly productivity has been found to increase with increase in the value of water depth during off sunshine hours (night). It has been found to occur due to the fact that the value of potable water yield decreases with increase in depth of water during sunshine hours which in turn occurs due to lower rise in temperature and hence lower temperature difference between water surface and inner surface of glass cover. During off sunshine hours, a reverse phenomenon has been witnessed because potable water yield increases due to higher heat content of water mass and hence higher sensible heat.

The plot of average daily productivity with depth of water for N-PVT-FPC-SS has been shown in Fig. 18. The value of average daily productivity for N-PVT-FPC-SS has been found to be almost constant beyond 1.4 m water depth. It suggests that 1.4 m can be taken as the optimum depth for N-PVT-FPC-SS on the basis of average daily productivity. It has been found to occur because both potable water yield and electricity gain remain almost constant beyond 1.4 m water depth.

7. Conclusions

The performance analysis of N-PVT-FPC-SS has been carried out by incorporating the variation of water depth. Two months namely June (simmer) and January (winter) have been considered for the analysis. Hourly thermal efficiency, hourly exergy efficiency, hourly overall exergy efficiency, hourly overall thermal efficiency and hourly productivity have been found to decrease with the increase in water depth. The optimum value of water depth has been found to be 1.40 m on the basis of average daily thermal efficiency, average daily exrgy efficiency, average daily overall exergy efficieny and average daily productivity.

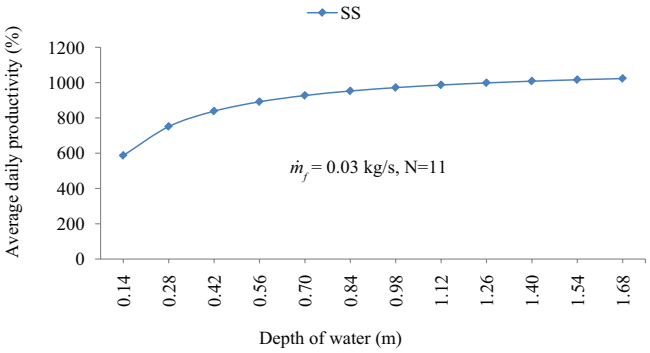

Fig. 18. Variation of average daily productivity with depth of water for N-PVT-FPC-SS.

Table 3
Uniform end-of-year annual cost for N-PVT-FPC-SS

n	i	P_s	M	S_s	$F_{CR,i,n}$	$F_{SR,i,n}$	UAC
Yr.	%	₹	₹	₹	Fraction	Fraction	₹
50	2	126,141.28	12,614.13	82,895	0.03182	0.01182	3,435.38
50	5	125,007.23	12,500.72	82,895	0.05478	0.00478	7,136.45
50	10	124,256.59	12,425.66	82,895	0.10086	0.00086	13,714.48

Symbols

A_b	—	Area of basin, m²
A_g	—	Area of glass cover, m²
C	—	Specific heat capacity, J/kg K
SS	—	Single slope solar still
ETC	—	Evacuated tubular collector
FF	—	Fill factor, dimensionless
F'	—	Collector efficiency factor, dimensionless
$\dot{E}x_{out}$	—	Hourly exergy output from single slope active solar still
$\dot{E}x_c$	—	Hourly exergy gain from *N* identical FPCs
FPC	—	Flat plate collector
HTC	—	Heat transfer coefficient
h_{cwg}	—	Convective HTC from water to inner surface of glass cover, W/m² K
h_{ewg}	—	Evaporative HTC from water surface to inner surface of glass cover, W/m² K
h_{ba}	—	HTC from blackened surface to water mass, W/m² K
h_{bw}	—	HTC from blackened surface to water mass, W/m² K
h_{rwg}	—	Radiative HTC from water surface to inner surface of glass cover, W/m² K
h_r	—	Radiative HTC, W/m² K
h_{1w}	—	Total HTC from water surface to inner surface of glass cover, W/m² K
h_{1g}	—	Total HTC from outer surface of glass cover to ambient, W/m² K
$I(t)$	—	Solar intensity on collector, W/m²
$I_s(t)$	—	Solar intensity on glass cover, W/m²
i	—	Rate of interest
K	—	Thermal conductivity, W/m K
L_g	—	Thickness of glass, m
L	—	Latent heat, J/kg
L′	—	Length, m
$\dot{m}_f$	—	Mass flow rate of fluid/water, kg/s
$\dot{m}_{ew}$	—	Mass of distillate per hour from N-ETC-SS/N-ETC-DS, kg
N-PVT-FPC-SS	—	Single slope solar still included with *N* identical PVT flat plate collectors
n	—	Life of N-PVT-CPC-SS, year
N	—	Number of collectors
PF_c	—	Penalty factor due to the glass covers for the glazed portion
PF_1	—	Penalty factor first, dimensionless
PF_2	—	Penalty factor second, dimensionless
PVT	—	Photovoltaic thermal
T_{foN}	—	Outlet water temperature at the end of *N*th water collector, °C
T_a	—	Ambient air temperature, °C
T_{gi}	—	Glass temperature at inner surface of glass cover, °C
T	—	Time, h
T_{wo}	_	Water temperature at $t = 0$, °C
T_w	_	Water temperature, °C
U_L	—	Overall heat transfer coefficient
V	—	Velocity of air, m/s

Subscript

eff	—	Effective
en	—	Energy
ex	—	Exergy
f	—	Fluid
g	—	Glass
in	—	Incoming
out	—	Outgoing
w	—	Water

Greek

α	—	Absorptivity (fraction)
η	—	Efficiency, %
$(\alpha\tau)_{eff}$	—	Product of effective absorptivity and transmittivity
σ	—	Stefan–Boltzmann constant, W/m² K⁴
τ	—	Transmittivity
β_c	—	Packing factor of module

References

[1] G.M. Zaki, T. El Dali, H. El Shafie, Improved Performance of Solar Still, Proc. First Arab Int. Solar Energy Conf., Kuwait, pp. 331–335.

[2] S.N. Rai, G.N, Tiwari, Single basin solar still coupled with flat plate collector, Energy Convers. Manage., 23 (1983) pp. 145–149.

[3] R. Sathyamurthy, S.A. El-Agouz, P.K. Nagarajan, J. Subramani, T. Arunkumar, D. Mageshbabu, B. Madhu, R. Bharathwaaj, N. Prakashe, A review of integrating solar collectors to solar still, Renew. Sustain Energy Rev., 77 (2017) 1069–1097.

[4] M. Tiana, Y. Sua, H. Zheng, G. Peic, G. Lic, S. Riffata, A review on the recent research progress in the compound parabolic concentrator (CPC) for solar energy applications, Renew. Sustain Energy Rev., 82 (2018) 1272–1296.

[5] Z.S. Abdel-Rehim, A. Lasheen, Experimental and theoretical study of a solar desalination system located in Cairo, Egypt, Desalination, 217 (2007) 52–64.

[6] O.A. Hamadou, K. Abdellatif, Modeling an active solar still for sea water desalination process optimization, Desalination, 354 (2014) 1–8.

[7] A.A. Badran, A.A. Al-Hallaq, I.A. Eyal Salman, M.Z. Odat, A solar still augmented with a flat-plate collector, Desalination, 172 (2005) 227–234.

[8] H. Taghvaei, H. Taghvaei, K. Jafarpur, M.R. Karimi Estahbanati, M. Feilizadeh, M. Feilizadeh, A.S. Ardekani, A thorough investigation of the effects of water depth on the performance of active solar stills, Desalination, 347 (2014) 77–85.

[9] F. Calise, M.D. d'Accadia, A. Piacentino, A novel solar trigeneration system integrating PVT (photovoltaic/thermal collectors) and SW (seawater) desalination: dynamic simulation and economic assessment, Energy, 67 (2014) 129–148.

[10] A.G.M. Ibrahim, E.E. Allam, S.E. Elshamarka, A modified basin type solar still: experimental performance and economic study, Energy, 93 (2015) 335–342.

[11] G.N. Tiwari, J.K. Yadav, D.B. Singh, I.M. Al-Helal, A.M. Abdel-Ghany, Exergoeconomic and enviroeconomic analyses of partially covered photovoltaic flat plate collector active solar distillation system, Desalination, 367 (2015) 186–196.

[12] D.B. Singh, J.K. Yadav, V.K. Dwivedi, S. Kumar, G.N. Tiwari, I.M. Al-Helal, Experimental studies of active solar still integrated with two hybrid PVT collectors, Solar Energy, 130 (2016) 207–223.

[13] S. Kumar, A. Tiwari, Design, fabrication and performance of a hybrid photovoltaic/thermal (PVT) active solar still, Energy Convers. Manage., 51 (2010) 1219–1229.

[14] D.D.W. Rufuss, V.R. Kumar, L. Suganthi, S. Iniyan, P.A. Davies, Techno-economic analysis of solar stills using integrated fuzzy analytical hierarchy process and data envelopment analysis, Solar Energy, 159 (2018) 820–833.

[15] S. Rashidi, J.A. Esfahani, N. Rahbar, Partitioning of solar still for performance recovery: experimental and numerical investigations with cost analysis, 153 (2017) 41–50.

[16] L. Malaeb, K. Aboughali, G.M. Ayoub, Modeling of a modified solar still system with enhanced productivity, Solar Energy, 125 (2016) 360–372.
[17] K. Rabhia, R. Nciria, F. Nasria, C. Alia, H.B. Bachae, Experimental performance analysis of a modified single-basin single-slope solar still with pin fins absorber and condenser, Desalination, 416 (2017) 86–93.
[18] S.W. Sharshir, G. Peng, N. Yang, M.A. Eltawil, M.K.A. Ali, A.E. Kabeel, A hybrid desalination system using humidification-dehumidification and solar stills integrated with evacuated solar water heater, Energy Convers. Manage., 124 (2016) 287–296.
[19] The Bao Nguyen, Factors affecting the yield of solar distillation systems and measures to improve productivity, Desal. Wat. Treat., 68 (2018) 91–98.
[20] S.J.P. Gnanaraj, S. Ramachandran, Optimization on performance of single-slope solar still linked solar pond via Taguchi method, Desal. Wat. Treat., 80 (2017) 27–40.
[21] Y.P. Yadav A.K. Singh, Experimental and theoretical investigations on a double exposure, Desal. Wat. Treat., 61 (2017) 257–261.
[22] M.A. Eltawil, Z.M. Omara, Enhancing the solar still performance using solar photovoltaic, flat plate collector and hot air, Desalination, 349 (2014) 1–9.
[23] F. Saeedi, F. Sarhaddi, A. Behzadmehr, Optimization of a PV/T (photovoltaic/thermal) active solar still, Energy, 87 (2015) 142–152.
[24] D.B. Singh, G.N. Tiwari, Effect of energy matrices on life cycle cost analysis of partially covered photovoltaic compound parabolic concentrator collector active solar distillation system, Desalination, 397 (2016) 75–91.
[25] D.B. Singh, G.N. Tiwari, Enhancement in energy metrics of double slope solar still by incorporating N identical PVT collectors, Solar Energy, 143 (2017) 142–161.
[26] D.B. Singh, G.N. Tiwari, Performance analysis of basin type solar stills integrated with N identical photovoltaic thermal (PVT) compound parabolic concentrator (CPC) collectors: a comparative study, Solar Energy, 142 (2017) 144–158.
[27] D.B. Singh, G.N. Tiwari, Exergoeconomic, enviroeconomic and productivity analyses of basin type solar stills by incorporating N identical PVT compound parabolic concentrator collectors: a comparative study, Energy Convers. Manage., 135 (2017) 129–147.
[28] R.V. Singh, S. Kumar, M.M. Hasan, M.E. Khan, G.N. Tiwari, Performance of a solar still integrated with evacuated tube collector in natural mode, Desalination, 318 (2013) 25–33.
[29] S. Kumar, A. Dubey, G.N. Tiwari, A solar still augmented with an evacuated tube collector in forced mode, Desalination, 347 (2014) 15–24.
[30] D.B. Singh, G.N. Tiwari, Analytical characteristic equation of N identical evacuated tubular collectors integrated single slope solar still, Desal. Wat. Treat., 88 (2017) 41–51.
[31] D.B. Singh, G.N. Tiwari, Energy, exergy and cost analyses of N identical evacuated tubular collectors integrated basin type solar stills: a comparative study, Solar Energy, 155 (2017) 829–846.
[32] T. Arunkumar, R. Velraj, D.C. Denkenberger, R. Sathyamurthy, K.V. Kumar, A. Ahsan, Productivity enhancements of compound parabolic concentrator tubular solar stills, Renew. Energy, 88 (2016) 391–400.
[33] S. Dubey, G.N. Tiwari, Analysis of PV/T flat plate water collectors connected in series, Solar Energy, 83 (2009) 1485–1498.
[34] Shyam, G.N. Tiwari, I.M. Al-Helal, Analytical expression of temperature dependent electrical efficiency of N-PVT water collectors connected in series, Solar Energy, 114 (2015) 61–76.
[35] D.L. Evans, Simplified method for predicting PV array output, Solar Energy, 27 (1981) 555–560.
[36] T. Schott, Operational Temperatures of PV Modules, Proceedings of 6th PV Solar Energy Conference, pp. 392–396.
[37] J. Fernandez, N. Chargoy, Multistage indirectly heated solar still, Solar Energy, 44 (1990) 215.
[38] S. Toyama, K. Kagakuv, Gijitsu, 24, 159, Maruzen, Tokyo, 1972.
[39] G.N. Tiwari, Solar Energy, Fundamentals, Design, Modeling and Application, Narosa Publishing House, 2013, pp. 278–306.
[40] P.K. Nag, Basic and Applied Thermodynamics, Tata McGraw-Hill, New Delhi, 2004.
[41] P.I. Cooper, Digital simulation of experimental solar still data, Solar Energy, 14 (1973) 451.
[42] R.V. Dunkle, Solar Water Distillation, the Roof Type Solar Still and Multi effect Diffusion Still, International Developments in Heat Transfer, A.S.M.E. Proc. International Heat transfer, Part V, p. 895, University of Colorado, 1961.
[43] R. Petela, Exergy of undiluted thermal radiation, Solar Energy, 86 (2003) 241–247.
[44] B.J. Huang, T.H. Lin, W.C. Hung, F.S. Sun, Performance evaluation of solar photovoltaic/thermal systems, Solar Energy, 70 (2001) 443–448.
[45] International Labor Office, Introduction to Work Study, International Labor Organization, Geneva, 1979.

Appendix A

Expressions for various terms used in Eqs. (1) and (2) are as follows:

$$U_{\text{tca}} = \left[\frac{1}{h_o} + \frac{L_g}{K_g}\right]^{-1};\quad U_{\text{tcp}} = \left[\frac{1}{h_i} + \frac{L_g}{K_g}\right]^{-1};$$

$$h_o = 5.7 + 3.8V, \text{W m}^{-2}\ \text{K}^{-1};\quad h_i = 5.7, \text{W m}^{-2}\ \text{K}^{-1};$$

$$U_{\text{tpa}} = \left[\frac{1}{U_{\text{tca}}} + \frac{1}{U_{\text{tcp}}}\right]^{-1} + \left[\frac{1}{h_i^{'}} + \frac{1}{h_{\text{pf}}} + \frac{L_i}{K_i}\right]^{-1};$$

$$h_i^{'} = 2.8 + 3V, \text{W m}^{-2}\text{K}^{-1};$$

$$U_{L1} = \frac{U_{\text{tcp}}U_{\text{tca}}}{U_{\text{tcp}} + U_{\text{tca}}};\quad U_{L2} = U_{L1} + U_{\text{tpa}};$$

$$U_{\text{Lm}} = \frac{h_{\text{pf}}U_{L2}}{F'h_{\text{pf}} + U_{L2}};\quad U_{\text{Lc}} = \frac{h_{\text{pf}}U_{\text{tpa}}}{F'h_{\text{pf}} + U_{\text{tpa}}};$$

$$PF_1 = \frac{U_{\text{tcp}}}{U_{\text{tcp}} + U_{\text{tca}}};\quad PF_2 = \frac{h_{\text{pf}}}{F'h_{\text{pf}} + U_{L2}};$$

$$\text{PF}_c = \frac{h_{\text{pf}}}{F'h_{\text{pf}} + U_{\text{tpa}}};\quad (\alpha\tau)_{1\text{eff}} = (\alpha_c - \eta_c)\tau_g\beta_c;$$

$$(\alpha\tau)_{2\text{eff}} = \alpha_p\tau_g^2(1-\beta_c);\quad (\alpha\tau)_{\text{meff}} = \left[(\alpha\tau)_{2\text{eff}} + PF_1(\alpha\tau)_{1\text{eff}}\right];$$

$$(\alpha\tau)_{\text{ceff}} = PF_c.\alpha_p\tau_g;\quad A_m = WL_m;\quad A_c = WL_c;$$

$$A_cF_{\text{Rc}} = \frac{\dot{m}_fc_f}{U_{\text{Lc}}}\left[1 - \exp\left(\frac{-F'U_{\text{Lc}}A_c}{\dot{m}_fc_f}\right)\right];$$

$$A_mF_{\text{Rm}} = \frac{\dot{m}_fc_f}{U_{\text{Lm}}}\left[1 - \exp\left(\frac{-F'U_{\text{Lm}}A_m}{\dot{m}_fc_f}\right)\right];$$

$$\left(AF_R(\alpha\tau)\right)_1 = \left[A_cF_{\text{Rc}}(\alpha\tau)_{\text{ceff}} + PF_2(\alpha\tau)_{\text{meff}}A_mF_{\text{Rm}}\left(1 - \frac{A_cF_{\text{Rc}}U_{\text{Lc}}}{\dot{m}_fc_f}\right)\right];$$

$$\left(AF_RU_L\right)_1 = \left[A_cF_{\text{Rc}}U_{\text{Lc}} + A_mF_{\text{Rm}}U_{\text{Lm}}\left(1 - \frac{A_cF_{\text{Rc}}U_{\text{Lc}}}{\dot{m}_fc_f}\right)\right];$$

$$K_K = \left(1 - \frac{(AF_RU_L)_1}{\dot{m}_fc_f}\right);\quad \left(AF_R(\alpha\tau)\right)_{m1} = PF_2(\alpha\tau)_{\text{meff}}A_mF_{\text{Rm}};$$

$$\left(AF_RU_L\right)_{m1} = A_mF_{\text{Rm}}U_{\text{Lm}};\quad K_m = \left(1 - \frac{A_mF_{\text{Rm}}U_{\text{Lm}}}{\dot{m}_fc_f}\right);$$

$$(\alpha\tau)_{\text{eff},N} = \frac{\left(AF_R(\alpha\tau)\right)_1}{(A_c + A_m)}\left[\frac{1-(K_K)^N}{N(1-K_K)}\right];$$

$$U_{L,N} = \frac{(AF_RU_L)_1}{(A_c + A_m)}\left[\frac{1-(K_K)^N}{N(1-K_K)}\right]$$

Expressions for a and $f(t)$ used in Eq. (4) and expressions of heat transfer coefficients used in Eqs. (5)–(7) are as follows:

$$a = \frac{1}{M_wC_w}\left[\dot{m}_fC_f\left(1-K_k^N\right) + U_sA_b\right];$$

$$f(t) = \frac{1}{M_wC_w}\left[\begin{array}{c}\alpha_{\text{eff}}^{'}\ A_b\bar{I}_s(t) + \dfrac{\left(1-K_k^{\ N}\right)}{(1-K_k)}(AF_R(\alpha\tau))_1\bar{I}_c(t) \\ + \left(\dfrac{\left(1-K_k^{\ N}\right)}{(1-K_k)}\left(AF_RU_L\right)_1 + U_sA_b\right)\bar{T}_a\end{array}\right];$$

$$\alpha_{\text{eff}}^{'} = \alpha_w^{'} + h_1\alpha_b^{'} + h_1^{'}\alpha_g^{'};\quad h_1 = \frac{h_{\text{bw}}}{h_{\text{bw}} + h_{\text{ba}}};$$

$$h_1^{'} = \frac{h_{1\text{w}}A_g}{U_{c,\text{ga}}A_g + h_{1w}A_b};\quad h_{1w} = h_{\text{rwg}} + h_{\text{cwg}} + h_{\text{ewg}};$$

$$h_{\text{ewg}} = 16.273\times10^{-3}h_{\text{cwg}}\left[\frac{P_w - P_{\text{gi}}}{T_w - T_{\text{gi}}}\right];$$

$$h_{\text{cwg}} = 0.884\left[\left(T_w - T_{\text{gi}}\right) + \frac{\left(P_w - P_{\text{gi}}\right)\left(T_w + 273\right)}{268.9\times10^3 - P_w}\right]^{\frac{1}{3}};$$

$$P_w = \exp\left[25.317 - \frac{5144}{T_w + 273}\right];\quad P_{\text{gi}} = \exp\left[25.317 - \frac{5144}{T_{\text{gi}} + 273}\right];$$

$$h_{\text{rwg}} = \left(0.82\times5.67\times10^{-8}\right)\left[(T_w + 273)^2 + (T_{\text{gi}} + 273)^2\right]\left[T_w + T_{\text{gi}} + 546\right];$$

$$U_s = U_t + U_b;\ U_b = \frac{h_{\mathrm{ba}} h_{\mathrm{bw}}}{h_{\mathrm{bw}} + h_{\mathrm{ba}}};\ U_t = \frac{h_{1w} U_{c,\mathrm{ga}} A_g}{U_{c,\mathrm{ga}} A_g + h_{1w} A_b};$$

$$h_{\mathrm{cb}} + h_{\mathrm{rb}} = 5.7\ \mathrm{W\ m^{-2}\ K^{-1}},\quad h_{\mathrm{bw}} = 250\ \mathrm{W\ m^{-2}\ K^{-1}};$$

$$U_{c,\mathrm{ga}} = \frac{\frac{K_g}{l_g} h_{1g}}{\frac{K_g}{l_g} + h_{1g}};\quad h_{\mathrm{ba}} = \left[\frac{L_i}{K_i} + \frac{1}{h_{cb} + h_{rb}} \right]^{-1};$$